Materials and Design xxx (2011) xxx–xxx

Contents lists available at ScienceDirect

Materials and Design

journal homepage: www.elsevier.com/locate/matdes

Stability, thermal and mechanical properties of Pt_xAl_y compounds

J. Feng [a,b,*], B. Xiao [b], J. Chen [a,*], Y. Du [a], J. Yu [a], R. Zhou [a]

[a] Key Laboratory of Advanced Materials of Precious-Nonferrous Metals, Education Ministry of China, and Key Lab of Advanced Materials of Yunnan Province, Kunming University of Science and Technology, Kunming 650093, PR China
[b] Department of Physics, School of Science and Engineering, Tulane University, LA 70118, USA

ARTICLE INFO

Article history:
Received 26 October 2010
Accepted 17 February 2011
Available online xxxx

Keywords:
Intermetallics
Mechanical
Elastic behavior

ABSTRACT

The stability, thermal and mechanical properties of Pt_xAl_y intermetallic compounds are investigated by density functional theory (DFT). The cohesive energy and formation enthalpy of Pt_xAl_y phases show that they are thermodynamically stable structures and these are in good agreement with the experiments. The heat capacity of the compounds is calculated by quasi-harmonic approximation (QHA) method. The thermal expansion coefficient as a function of temperature for each compound is also discussed. The elastic properties such as bulk modulus, Young's modulus are evaluated by Viogt–Reuss–Hill approximation. The anisotropic properties of sound velocities for the Pt_xAl_y compounds are explored. The calculated Poisson's ratio varies from 0.26 to 0.39 for Pt_xAl_y phases and the bonds in the compounds are mainly metallic and covalent types.

1. Introduction

Platinum and its alloys have been applied to many important industrial fields, such as catalysts, high temperature structural materials, special solder and shape memory alloys. Nevertheless, the physical and chemical properties of intermetallics of many noble metals are usually unknown because it is difficult to obtain sufficient samples of such compounds for the experiments [1,2]. One of important application of Pt based alloy is the bonding coat for thermal barrier coatings where it can be used to protect the heat resistance devices [3]. Nickel-based (Ni) superalloys are prevalently used in high temperature structural materials and corrosion resistance materials [4–6]. However, the standards of high temperature properties of structural materials are rising and the nickel-based superalloys cannot meet the requirements [7]. Platinum and Pt_xAl_y compounds, with their remarkable high-temperature strengths, have been extensively investigated, which have outstanding properties such as good diffusional creep resistance, high-temperature strength, high melting points and good oxidation resistance [8]. Nevertheless, the stabilities, mechanical properties of these compounds are incomplete and disputable [8]. The formation enthalpy of Pt_xAl_y binary compounds in the composition range of 17.7–74.7 at.% Platinum has been determined [9]. The Al–Pt binary phase diagram by experiments have been reported [10,11]. The phase diagram Al–Pt system has been calculated by using the CALPHAD method, but two important Pt_3Al phases are omitted [12,13]. Comparing the two phase diagrams [10–12], the results [11] have referred more metastable phases than CALPHAD results [8], such as β phase, low temperature phase of Pt_2Al and Pt_3Al. The intermetallic compounds Pt_5Al_{21}, Pt_8Al_{21}, $PtAl_2$, Pt_2Al_3, PtAl, Pt_5Al_3, Pt_2Al and Pt_3Al were treated as stoichiometric compounds in Pt–Al binary system [14]. Thermodynamic databases for several Platinum binary compounds have been developed [13–15]. By using the electron beam vacuum deposition to prepare Pt–Al alloys with different compositions, the obtained samples have been annealed in a standard vacuum furnace to fabricate various Pt_xAl_y phases, and the formation enthalpies of them have been successfully obtained [15]. References have reported the electronic properties and stability of four Pt_3Al polymorphs by *ab initio* method, and found that LT-Pt_3Al is the most stable phase among four polymorphs which has the smallest formation enthalpy value [15–17]. A detailed description of the electronic structures, stability, elastic constants and thermal properties of Pt_xAl_y binary compounds using first principles calculations are not carried out all the time. The information provide by such investigations will be extremely useful for developing the Pt–Al superalloys. Therefore, the first principles calculations are performed in this paper for the most Pt_xAl_y binary compounds, and the electronic structures, elastic constants, thermal expansion properties and stabilities of them are calculated and discussed.

2. Methods and details

The whole calculations have been carried out using first principle calculations which are based on density functional theory as

* Corresponding authors at: Key Laboratory of Advanced Materials of Precious-Nonferrous Metals, Education Ministry of China, and Key Lab of Advanced Materials of Yunnan Province, Kunming University of Science and Technology, Kunming 650093, PR China. (J. Feng) Tel.: +86 08715189490; fax: +86 08715334185.
E-mail addresses: fengj09@mails.tsinghua.edu.cn (J. Feng), chenjingchao@kmust.edu.cn (J. Chen).

0261-3069/$ - see front matter © 2011 Elsevier Ltd. All rights reserved.
doi:10.1016/j.matdes.2011.02.043

implemented in CASTEP code [18–20]. Ultrasoft pseudo potentials were used to represent the interactions between ionic core and valence electrons. The exchange correction energy was calculated by the generalized gradient-corrected (GGA) function developed by Perdew, Burke, and Ernzerhof (PBE) [21]. The total energy changes during the optimization process were finally converged to 1×10^{-6} eV and the force per atom was reduced to 0.01 eV/Å. Monkhorst–Pack scheme was used for **k**-point sampling in the first irreducible Brillouin zone (BZ), as $10 \times 10 \times 10$ for all structures. Valence electron configurations included in this study are Al: $3s^2$ $3p^1$ and Pt: $5d^9$ $6s^1$. Pulay density mixing scheme was applied for the electron energy minimization process. The maximum energy cutoff value was 450.0 eV for plane wave expansions. The elastic constants of the compounds in Al–Pt binary system were calculated using the stress-strain relations, namely Hooker's law, and in which several different strain modes were imposed on the crystal structure, and then the Cauchy stress tensor for each strain mode was evaluated and then the related elastic constants were identified as the coefficients in strain–stress relations as shown in Eq. (1).

$$\begin{pmatrix} \sigma_1 \\ \sigma_2 \\ \sigma_3 \\ \tau_4 \\ \tau_5 \\ \tau_6 \end{pmatrix} = \begin{pmatrix} C_{11} & C_{12} & C_{13} & C_{14} & C_{15} & C_{16} \\ & C_{22} & C_{23} & C_{24} & C_{25} & C_{26} \\ & & C_{33} & C_{34} & C_{35} & C_{36} \\ & & & C_{44} & C_{45} & C_{46} \\ & & & & C_{55} & C_{56} \\ & & & & & C_{66} \end{pmatrix} \begin{pmatrix} \varepsilon_1 \\ \varepsilon_2 \\ \varepsilon_3 \\ \gamma_4 \\ \gamma_5 \\ \gamma_6 \end{pmatrix} \quad (1)$$

where, C_{ij} is the elastic constant, τ_i and σ_i are the shear stress and normal stress, respectively. The total number of independent elastic constants is determined by the symmetry of the crystal, and for high symmetry point group, the required different strain patterns for the C_{ij} calculations can be greatly reduced, for example, one can obtain the full set elastic constants of cubic crystal using one strain pattern.

In order to estimate the relative stability of Pt_xAl_y compounds, the cohesive energy and formation enthalpy were also studied in this paper, the following expressions (Eq. (2) and (3)) were used for their calculations.

$$E_{coh}(Pt_xAl_y) = \frac{E_{total}(Pt_xAl_y) - xE_{iso}(Pt) - yE_{iso}(Al)}{x+y} \quad (2)$$

$$\Delta_r H_m(Pt_xAl_y) = \frac{E_{total}(Pt_xAl_y) - xE_{bulk}(Pt) - yE_{bulk}(Al)}{n} \quad (3)$$

Here, $E_{coh}(Pt_xAl_y)$ and $\Delta_r H_m(Pt_xAl_y)$ is the cohesive energy and formation enthalpy, respectively; E_{iso} refers to the total energy of an isolated Al or Pt atom; $E_{total}(Pt_xAl_y)$ is the total cell energy and E_{bulk} is the chemical potential of Al or Pt atom in the bulk state, and n represents the total number of formula per cell. In the present study, we built a large cubic cell (a = 1 nm) and placed one Al or Pt atom in the center of the cell and then calculated E_{iso} value. The ground state crystal structures of Al and Pt were used for the chemical potential calculations.

3. Results and discussions

3.1. Stability

Fig. 1 shows the crystal structures of the Pt_xAl_y binary compounds investigated in this paper. The Pt_xAl_y binary compounds have a large number of different lattice types, including cubic, trigonal, tetragonal and orthorhombic crystal classes which are determined by the temperature and composition, for instance both Pt_2Al and Pt_3Al have low and high temperature polymorphs (Table 1). The chemical stability of the intermetallic compounds in the Al–Pt binary system can be described by cohesive energy and

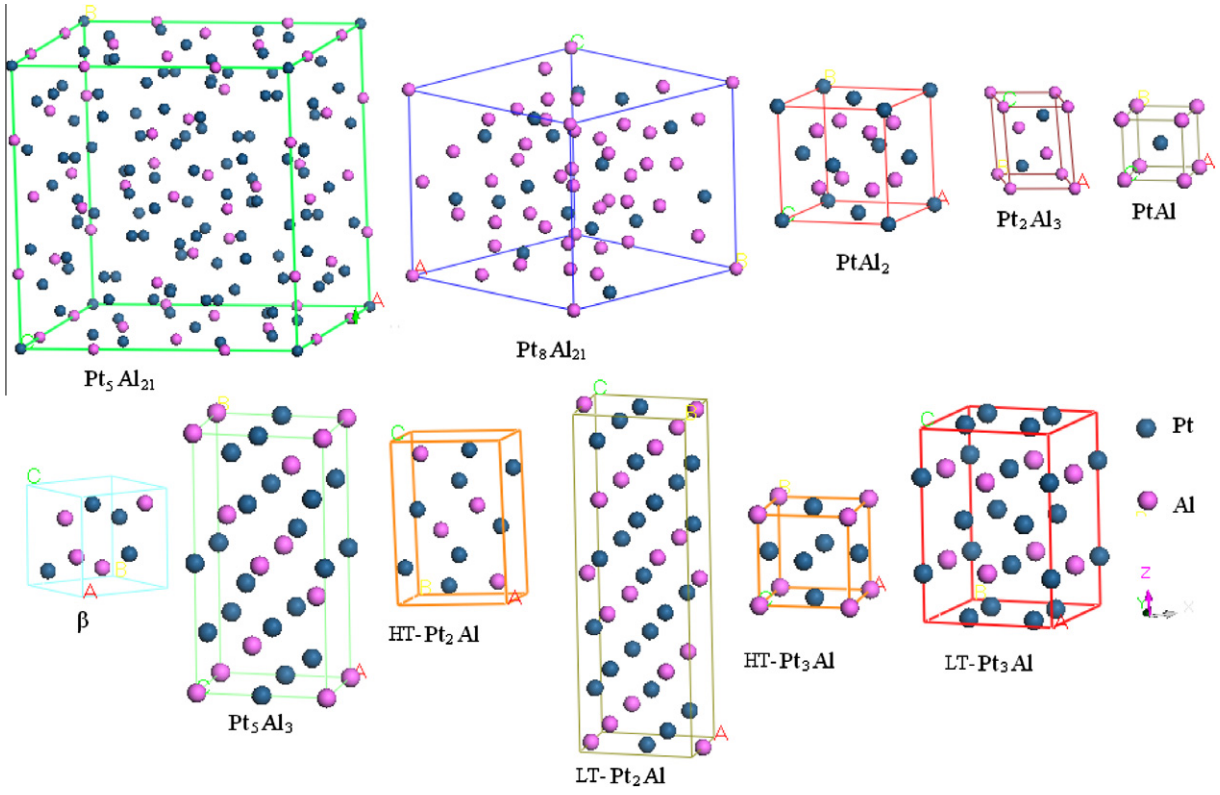

Fig. 1. The crystal structures of the intermetallic compounds in Al-Pt binary system.

Please cite this article in press as: Feng J et al. Stability, thermal and mechanical properties of Pt_xAl_y compounds. J Mater Design (2011), doi:10.1016/j.matdes.2011.02.043

formation enthalpy. As can be seen from Table 2, the cohesive energy decreases by increasing the Pt content in Pt_xAl_y, the maximum and minimum value is −3.861 eV/atom and −6.463 eV/atom for Al and Pt crystal, respectively. The cohesive energy of light elements is usually smaller than that of heavy transition metals due to quite different valence structures. Therefore, Pt is more stable than Al in ground state from the point view of cohesive energy, which is in agreement with experiments [22]. The stability of the compound is determined by the formation enthalpy (Eq. (3)), therefore the negative value for formation enthalpy is expected for the stable crystal. Fig. 2 depicts the calculated and previously reported formation enthalpies of Pt_xAl_y compounds [23–29]. The calculated values are in agreement with the experiments. For the most compounds, the theoretical values are larger than experimental results, because GGA was used throughout the calculations. One should also note that the theoretical values are all obtained at 0 K rather than at room temperature for experimental results. The discrepancies between them may or may not be due to the temperature effect only; many other factors are also possible, such as defects in real materials. In addition, the formation enthalpies of HT (High temperature)/LT (Low temperature) – Pt_3Al polymorphs are agree well with the values reported by de Waal and Pretorius [15] and Chauke et al. [16]. No positive value is observed which clearly indicates that all of the considered compounds are thermodynamically stable and can be synthesized easily by conventional methods. The increment of Pt content in Pt_xAl_y compounds produces a nearly parabolic curve for formation enthalpy as illustrated in Fig. 1. The two phases of PtAl have the smallest formation enthalpies among the studied Pt_xAl_y binary compounds. The formation enthalpy of PtAl and β-PtAl is very close to each other, the difference is only 0.1 kJ/mol. Furthermore, the calculated cohesive energy clear shows that PtAl is more stable than β phase, and which is in good agreement with formation enthalpy sequence obtained [12]. Interestingly, the relative stability of the two Pt_3Al phases, namely HT-Pt_3Al and LT-Pt_3Al, are not definitely confirmed, because the obtained cohesive energy and formation enthalpy have opposite trends; moreover, the difference of the formation enthalpy between the two crystals is not large enough to exclude the less stable one. Four different possible crystal structures of Pt_3Al were investigated using CASTEP code, and both the formation enthalpy and phonon spectrum of them were calculated [16]. The results clearly showed that the LT-Pt_3Al is the most stable structure among four crystals which has the smallest formation enthalpy, and both HT-Pt_3Al and LT-Pt_3Al are dynamically stable as the full phonon spectrums are all positive values. However, we also note that in their calculations, HT-Pt_3Al is the most unstable phase, showing the largest enthalpy value. In addition, both references pointed out that the LT-Pt_3Al is rarely observed in experiments and the exact crystal structures of Pt_3Al phases are still unclear [11,12]. Based on these arguments, we conjecture that HT-Pt_3Al is stable or at least the stability of it is comparable to LT-Pt_3Al, and this will be explained from electronic aspect. Although the cohesive energy of Pt is much smaller than Al, a large formation enthalpy of the Pt_xAl_y compounds is not with higher Pt content [14,16,23]. As can be seen from Fig. 1, the enthalpy dates in the present paper are in agreement with the other theoretical and experimental results; all of these curves reflect the most stable phase is PtAl. According to the Hume–Rothery's rules on the formation of solid solution between two distinct elements, the atomic size, crystal structure and electronic structure play important roles in forming a continuous solid solution. In the binary Al–Pt system, the electronic structure decides the crystal structures of the intermetallics. The atomic radii of Pt and Al are 0.138 nm and 0.143 nm, respectively. The difference is smaller than 10%, and both Al and Pt adopt the face centered cubic structures, implying that the continuous solid solution could be formed in theory. However, the electronic structure of Pt and Al are quite different from each other. In atomic state, the 2*p* level of Al has a lower energy than 5*d* and 6*s* orbitals of Pt, indicating that Al could accept valence electrons from Pt, as a result, the Pt–Al bond will show ionic character. In fact, the Hume–Rothery's rules for the electronic compounds can hardly be used to explain the complicated crystal structures of

Table 1
Wyckoff positions of Pt_xAl_y compounds.

Species	Pt				Al				Refs.
	Wyckoff positions	*x*	*y*	*z*	Wyckoff positions	*x*	*y*	*z*	
Pt_8Al_{21}	16f	0.407	0.130	0.095	4b	0	0	0.5	[23]
	16f	0.402	0.785	0.792	16f	0.447	0.589	0.400	
					16f	0.752	0.589	0.449	
					16f	0.781	0.789	0.525	
					16f	0.282	0.509	0.021	
					16f	0.407	0.429	0.228	
$PtAl_2$	4a	0	0	0	8c	0.25	0.25	0.25	[24]
Pt_2Al_3	2d	0.333	0.667	0.081	1a	0	0	0	[25]
	2d	0.333	0.667	0.581	1b	0	0	0.5	
					2c	0	0	0.25	
					2d	0.333	0.667	0.333	
PtAl	1b	0.5	0.5	0.5	1a	0	0	0	[26]
β	1b	0.5	0.5	0.5	1a	0	0	0	[10]
Pt_5Al_3	2c	0	0.5	0	2a	0	0	0	[25]
	4 g	0.09	0.235	0	4 h	0.34	0.15	0.5	
	4 h	0.30	0.39	0.5					
HT-Pt_2Al	4c	0.033	0.25	0.213	4c	0.72	0.25	0.59	[27]
	4c	0.169	0.25	0.570					
LT-Pt_2Al	4i	0.075	0	0.788	2b	0	0.5	0	[27]
	2d	0	0.5	0.5	4i	0.087	0	0.272	
	4j	0.16	0.5	0.047	2e	0.25	0	0.784	
	4j	0.164	0.5	0.549					
	2e	0.25	0	0.287					
HT-Pt_3Al	3c	0	0.5	0.5	1a	0	0	0	[25]
LT-Pt_3Al	4 g	0.241	0.741	0	4f	0.5	0	0.264	[10,16,17]
	4e	0	0	0.251					
	4 h	0.286	0.786	0.5					

Please cite this article in press as: Feng J et al. Stability, thermal and mechanical properties of Pt_xAl_y compounds. J Mater Design (2011), doi:10.1016/j.matdes.2011.02.043

Table 2
Crystal parameters, cohesive energy (E_c) and formation enthalpy (ΔH) of Pt_xAl_y compound.

Species	Methods	Temperature range (K)	Composition at.% Pt	Space Group	Lattice constants (Å)			E_c (cal.) (eV/atom)	ΔH (kJ/mol)	
					a	*b*	*c*			
Pt_5Al_{21}	Exp. Cal.	<928	~19.2	Pm-3 m (No.221)	*a* = *b* = *c* = 19.23[a]				−50.2[c]	−54.0[d]
					a = *b* = *c* = 19.15[b]			−5.007	50.2[e]	−55.1[b]
Pt_8Al_{21}	Exp. Cal.	<1082	~27.5	I41/A (No. 88)	*a* = *b* = *c* = 10.60[f]				−71.3[c]	−81.0[d]
					a = *b* = *c* = 10.49[b]			−5.397	−71.4[e]	−83.3[b]
$PtAl_2$	Exp. Cal.	<1400	~33.3	Fm-3 m (No.225)	*a* = *b* = *c* = 5.91[g]				−90.0[c]	−82.0[d]
					a = *b* = *c* = 5.84[b]			−5.696	−81.8[e]	−93.7[b]
Pt_2Al_3	Exp. Cal.	<1677	40	P-3m1 (No.164)	*a* = *b* = 4.208[h]		5.172		−94.9[c]	−96.0[d]
					a = *b* = 4.185[b]		5.140	−5.949	−84.9[e]	−97.5[b]
PtAl	Exp. Cal.	<1766	50	Pm-3 m (No.221)	*a* = *b* = *c* = 3.125[i]				−101[c]	−100[d]
					a = *b* = *c* = 3.043[b]			−6.112	−92.9[e]	−99.8[b]
β	Exp. Cal.	~1533–1783	~51–56	Pm-3 m (No.221)	*a* = *b* = *c* = 4.864[a]				−100[c]	–
					a = *b* = *c* = 4.868[b]			−5.831	−92.8[e]	−96.3[b]
Pt_5Al_3	Exp. Cal.	<1695	~62.5	Pbam (No. 55)	5.413[g]	10.73	3.950		−87.8[c]	−88.5[d]
					5.406[b]	10.72	3.975	−6.426	−87.4[e]	−90.8[b]
HT-Pt_2Al	Exp. Cal.	~<1398	~66.7	Pnma (62)	5.401[j]	4.055	7.898		−87.3[c]	–
					5.421[b]	4.073	7.864	−6.441	−83.4[e]	−90.4[b]
LT- Pt_2Al	Exp. Cal.	~1398–1750	~66.7	Pmma (No.51)	16.30[l]	3.921	5.439		−88.0[c]	–
					16.39[b]	3.908	5.459	−6.423	–	−90.8[b]
HT-Pt_3Al	Exp. Cal. Cal.	~1553–1835	~70.3–82.5	Pm-3 m (No.221)	*a* = *b* = *c* = 3.876[g]				−69.9[c]	−68.0[d]
					a = *b* = *c* = 3.863[k]				−76.6[k]	−74.3[e]
					a = *b* = *c* = 3.895[b]			−6.449	–	−70.2[b]
LT- Pt_3Al	Exp. Cal. Cal.	~<1553	~74.0–78.0	P4/mbm (No. 127)	*a* = *b* = 5.452[l]		*c* = 7.820		−71.1[l]	−70.2[m]
					a = *b* = 5.428[k]		c = 7.811		−77.2[k]	−76.2[e]
					a = *b* = 5.463[b]		*c* = 7.829	−6.186	–	−73.7[b]
Pt	Exp. Cal.	<2045	100	Fm-3 m (No.225)	*a* = *b* = *c* = 3.887[d]				0[d]	0[m]
					a = *b* = *c* = 3.924[b]			−6.063	0[e]	0[b]
Al	Exp. Cal.	<933.3	0	Fm-3 m (No.225)	*a* = *b* = *c* = 4.05[d]				0[m]	0[n]
					a = *b* = *c* = 4.05[b]			−3.861	0[e]	0[b]

[a] Exp. In Ref. [9].
[b] This work.
[c] Exp. In Ref. [10].
[d] Exp. In Ref. [15].
[e] Cal. In Ref. [12].
[f] Exp. In Ref. [23].
[g] Exp. In Ref. [24].
[h] Exp. In Ref. [25].
[i] Exp. In Ref. [26].
[j] Exp. In Ref. [27].
[k] Cal. In Ref. [16].
[l] Exp. In Ref. [17].
[m] Exp. In Ref. [28].
[n] Exp. In Ref. [29].

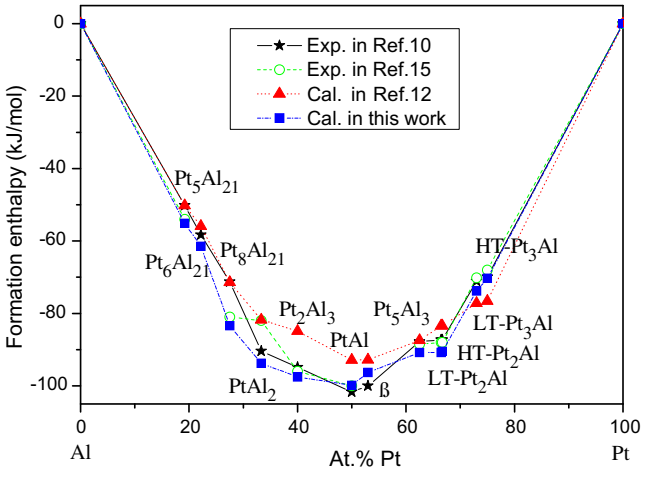

Fig. 2. The calculated formation enthalpy of Pt_xAl_y binary compounds, the values are compared with other experimental and theoretical results.

Pt_xAl_y compounds. The ability to form various binary compounds in Al–Pt system may originate from the electronic structures. When comparing with the Ni based superalloys, the melting point of the compounds in Al–Pt binary system is relatively high which may improve the mechanical performances of Pt_xAl_y alloy at high temperatures.

3.2. Mechanical properties

The elastic properties of the compound are usually characterized by the modulus, such as bulk modulus (B), Young's modulus (E) and shear modulus (G). They can be calculated with the elastic constants using Viogt–Reuss–Hill (VRH) approximation. The Voigt–Reuss–Hill approximation is an average of the two bounds, namely the lower bound of Voigt and upper bound of Reuss, which provides the best estimation for the mechanical properties of polycrystalline materials from the known elastic constants for single crystal (Eq. (4)–(9)) [30].

$$B_{VRH} = \frac{1}{2}(B_V + B_R) \tag{4}$$

$$G_{VRH} = \frac{1}{2}(G_V + G_R) \tag{5}$$

$$E = 9B_{VRH}G_{VRH}/(3B_{VRH} + G_{VRH}) \tag{6}$$

$$\sigma = \frac{(3B_{VRH} - 2G_{VRH})}{[2(3B_{VRH} + G_{VRH})]} \quad (7)$$

$$\lambda = \frac{\sigma E_{VRH}}{(1+\sigma)(1-2\sigma)} \quad (8)$$

$$\mu = \frac{E_{VRH}}{2(1+\sigma)} \quad (9)$$

where B_V, B_R and B_{VRH}, is the bulk modulus calculated by Voigt, Reuss and Voigt–Reuss–Hill approximation, respectively. G_V, G_R and G_{VRH}, is the shear modulus calculated by Voigt, Reuss and Voigt–Reuss–Hill approximation, respectively. E (or E_{VRH}) is the Young's modulus and σ is the Poisson's ratio, which is both calculated by Voigt–Reuss–Hill approximation. The calculation formulas in Voigt–Reuss–Hill method are dependent on the crystal symmetry, and which are all listed in present paper. The calculated full set elastic constants of the Pt_xAl_y binary compounds are shown in Table 3. The mechanical stability of the crystal under external stain can be estimated using Born–Huang criterion; these conditions are given as formulas [31]. One can easily find that all of the Pt_xAl_y compounds satisfy the corresponding stability conditions [31,32]. The obtained bulk modulus values of Pt and Al are in good agreement with other references, and the bulk modulus of Pt is significantly larger than that of Al. Therefore, substituting Al with Pt will increase the bulk modulus of Al alloys, and this is well known as solid solution strength. We can see that the elastic constants of Al rich compounds are greater than Al bulk such as C_{11}, C_{12} and C_{44}. On the other hand, the calculated elastic constants for Pt rich compounds are slightly lower or comparable to bulk Pt. As a result, the obtained B, G and E values of Pt_xAl_y binary compounds show similar trends as for the elastic constants. In this paper, we also evaluated the first and second order Lame constants, namely compressibility and shear stiffness, using the Eq. (8) and (9) [32]. The variations of the compressibility of Pt_xAl_y compounds are analogous to bulk modulus. PtAl has the largest stiffness value among all of the crystals because of the isotropic response to shear strain. Fig. 3 shows the variations of elastic parameters of Pt_xAl_y compounds. The E values of Pt_2Al_3 and PtAl are greater than other compounds, and the corresponding B/G ratios are small, because they have small Poisson's ratios. The chemical bonds in these two compounds may show more ionic features.

It is reported that for the compound $B/G < 1.75$, and for metallic compound that value is larger than 1.75, for example, diamond (0.8), Al (2.74), Co (2.43), Zr (1.74) and etc. The hardness and brittleness of the compound may relate to the B/G value, the compound with high hardness usually has small B/G value. In other words, if the B/G value of the compound is smaller than 2.0, the compound should be brittle. The correlation between the Vickers hardness and bond length is proposed to be $H_V \propto \frac{1}{d^6}$ for covalent crystals with partial iconicity [32]. The bulk modulus and shear modulus also have the similar relations with respect to bond length. Bulk modulus is proportional to $\frac{1}{d^{3.5}}$ and for shear modulus that is $\frac{1}{d^5}$. One may conclude that G is more closely related to hardness than the B. In this paper, besides the B/G, the G value is also used to indicate the hardness of the compound. Fig. 3 shows the calculated modulus and B/G for each compound, the B/G value is multiplied by the factor of 50 for a better illustration. The correlation between the C_{44} and shear modulus can be clearly seen in the Fig. 3, and such relationship between B and C_{44} is not simple. On the other hand, PtAl has the smallest B/G value and largest G value. Furthermore, though the content of Pt is higher than 50% in the compound, both the Young's modulus and shear modulus have a mutation in the Pt_5Al_3 compound. The reason may be the chemical bonds of these compounds before PtAl and β phase (the ratio of Pt and Al is 1:1) are similar with aluminum, on the contrary, the properties of the content of higher than 50%Pt in the compound are similar with platinum. The ductility of these compounds decreases with Pt content increasing before PtAl. Nevertheless, it increases by further enhancing the Pt concentrations, finally reaching the largest B/G value for Pt.

3.3. Debye temperature and anisotropic sound velocity

The calculations for elastic constants enable us to estimate the Debye temperature for each Pt_xAl_y compound; the expressions used are given by Eq. (10)–(12) [33].

$$\Theta_D = \frac{h}{k}\left[\frac{3n}{4\pi}\left(\frac{N_A\rho}{M}\right)\right]^{1/3} v_m \quad (10)$$

where, Θ_D represents Debye temperature; h and k is Planck and Boltzmann constant, respectively; N_A is the Avogadro's number, n is the number of atoms in the molecule, M is the molecular weight,

Table 3
The elastic constants (C_{ij}), bulk modulus (B), Yong's modulus (E), shear modulus (G), poisson's ratio (σ), the first order Lame constant (λ) and the second Lame constant (μ).

Species	C_{ij} (GPa)									G (GPa)	E (GPa)	B (GPa)	B/G	σ	λ (GPa)	μ (GPa)
	C_{11}	C_{44}	C_{12}	C_{23}	C_{55}	C_{22}	C_{33}	C_{66}	C_{13}							
Pt_8Al_{21}	246.7	73.2	103.5	–	–	–	215.5	62.96	91.85	69.84	180.3	142.1	2.035	0.289	95.7	69.9
$PtAl_2$	237.9	74.5	107.9	–	–	–	–	–	–	61.02	183.2	151.2	2.478	0.322	125.5	69.3
Pt_2Al_3	351.8	80.6	144.7	–	–	–	291.8	–	111.5	93.9	242	190.8	2.032	0.289	128.2	93.9
PtAl	361.2	103.2	128.7	–	–	–	–	–	–	108.2	276.4	206.2	1.906	0.277	134.1	108.2
β	315.4	80.0	136.6	–	–	–	–	–	–	82.9	230	198	2.388	0.316	150.4	87.4
Pt_5Al_3	284.1	58.1	157.4	185.6	87.8	285.1	286.6	67.79	204.6	60.93	167.1	216	3.545	0.371	175.4	60.9
HT-Pt_2Al	310.8	63.6	173.3	178.8	51.2	315.8	314.4	76.7	158.2	66.25	180.4	217.8	3.288	0.362	173.6	66.2
LT-Pt_2Al	309.1	108.6	171.6	170	69.5	317.5	366.5	110	143.8	89.1	236.1	217.2	2.438	0.320	158.4	89.5
HT-Pt_3Al	331.6	72.4	193.2	–	–	–	–	–	–	71.08	194	239.3	3.367	0.365	191.9	71.1
LT-Pt_3Al	398.8	111.9	162.8	–	–	–	386.2	63.9	214.0	94.3	273.2	262.5	2.784	0.335	199.6	97.0
LT-Pt_3Al[a]	396	120	158	–	–	–	361	49	210	–	–	256	–	–	–	–
Pt	358.8	62.3	191	–	–	–	–	–	–	71.23	192	246.9	3.466	0.368	196.4	70.2
Pt[b]	349.7	61	170.2	–	–	–	–	–	–	71.1	193	230	3.235	0.360	182.2	70.9
Al	106.8	29.31	56.95	–	–	–	–	–	–	27.5	73.3	73.6	2.676	0.334	55.2	27.5
Al[b]	101	31	50	–	–	–	–	–	–	28.7	75.3	67	2.334	0.313	47.8	28.7
Al[c]	107	28	61	–	–	–	–	–	–	26	70	76	2.923	0.346	58.6	26.0

[a] Ref. [16].
[b] Exp. in Ref. [29].
[c] Exp. in Ref. [33].

Please cite this article in press as: Feng J et al. Stability, thermal and mechanical properties of Pt_xAl_y compounds. J Mater Design (2011), doi:10.1016/j.matdes.2011.02.043

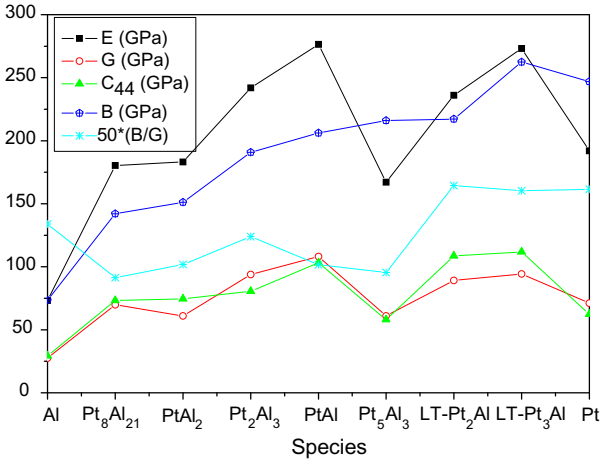

Fig. 3. The variations of the elastic parameters of Pt_xAl_y binary compounds and B/G ratios, note that B/G value is magnified by 50 times to the initial value.

and ρ is the density [30,33]. The average sound velocity v_m can be calculated using Eq. (11) and (12).

$$v_m = \left[\frac{1}{3}\left(\frac{2}{v_l^3}+\frac{1}{v_t^3}\right)\right]^{-\frac{1}{3}} \tag{11}$$

$$\begin{cases} v_l = \sqrt{(B+\frac{4}{3}G)/\rho} \\ v_t = \sqrt{G/\rho} \end{cases} \tag{12}$$

B and G are isothermal bulk modulus and shear modulus. v_l is the longitudinal sound velocity and v_t the transverse sound velocity. Table 4 shows the calculated Debye temperature and sound velocities of Pt_xAl_y binary compounds. Debye temperature reflects the strength of chemical binding in the crystal structure and which is inverse to the molecular weight. As a result, the Debye temperature of Al is larger than Pt. The similar results are also obtained for Al rich compounds in Al–Pt binary system. Both v_l and v_t are correlated to bulk modulus and density, the compound with low density and high bulk modulus will have large sound velocities. Because the density of bulk Pt is 21.45 g/cm^3, and which is near 10 times larger than bulk Al, so the calculated sound velocities of Al are obviously larger than Pt. The conclusion can be used to explain the sound velocities of other Pt_xAl_y compounds. It seems that the sound velocities are more strongly determined by density of the compound than bulk modulus. Since the thermal conductivity of the compound is proportional to the average sound velocity, thus one expect that Al rich compounds will show a good thermal conductivity, and Pt rich compounds will impede the transfer of heat energy.

The sound velocity in a solid is anisotropic which is determined by the symmetry of the crystal and propagation directions (Eq. (13) and (14)) [33].

$$|C_{ijkl}n_in_l - \rho v^2\delta_{ik}| = 0 \tag{13}$$

$$v(k) = \frac{d\omega}{dk} \tag{14}$$

For example, the pure transverse and longitudinal modes can only be found for [0 0 1], [1 1 0] and [1 1 1] directions in a cubic crystal and the sound propagating modes in other directions are the quasi-transverse or quasi-longitudinal waves. In this paper, we only consider the pure propagating modes for Pt_xAl_y binary compounds: [0 0 1], [1 1 0], [1 1 1] directions for cubic crystal; [0 0 1], [1 0 0] and [1 1 0] directions for tetragonal crystal; [1 0 0], [0 1 0] and [0 0 1] directions for orthorhombic crystal; [1 0 0] and [0 0 1] for trigonal crystal. The sound velocities are also related to elastic constants and phonon frequencies by Eqs. (15)–(25) in different directions for crystals, respectively [33,34].

Cubic crystal class:

$$[100] = [010] = [001] \quad \text{(polarization)}$$
$$[100]\, v_l = \sqrt{C_{11}/\rho}; \quad [010]\, v_{t1} = [001]\, v_{t2} = \sqrt{C_{44}/\rho}; \tag{15}$$
$$[110]$$
$$[110]\, v_l = \sqrt{(C_{11}+C_{12}+2C_{44})/2\rho}; \quad [1\bar{1}0]\, v_{t1} = \sqrt{(C_{11}-C_{12})/\rho};$$
$$[001]\, v_{t2} = \sqrt{C_{44}/\rho} \tag{16}$$
$$[111]$$
$$[111]\, v_l = \sqrt{(C_{11}+2C_{12}+4C_{44})/3\rho};$$
$$[11\bar{2}]\, v_{t1} = v_{t2} = \sqrt{(C_{11}-C_{12}+C_{44})/3\rho}; \tag{17}$$

Tetragonal crystal class:

Table 4
Sound velocity, Debye temperature (Θ_D) of Pt_xAl_y compound.

	ρ (g/cm^3)	v_l (m/s)	v_t (m/s)	v_m (m/s)	Θ_D (K)	$C_p = \gamma T + \beta' T^3$	
						γ	$\beta'(10^{-5})$
Pt_8Al_{21}	7.89	5459.8	2975.2	3318.5	395.7	6.21	13.10
$PtAl_2$	8.01	5388.1	2760.1	3091.7	355.6	5.76	6.10
Pt_2Al_3	9.86	5660.9	3086.0	3442.0	406.7	7.83	1.98
PtAl	12.1	5381.6	2990.3	3330.5	398.9	6.97	2.80
β	12.8	4909.4	2544.9	2848.5	347.6	5.88	3.59
Pt_5Al_3	15.29	4408.9	1996.2	2250.8	275.1	6.58	6.58
HT-Pt_2Al	16.02	4371.3	2033.6	2290.1	279.4	6.31	4.83
LT-Pt_2Al	15.95	4589.5	2363.5	2646.6	322.5	7.74	4.37
HT-Pt_3Al	17.46	4374.0	2017.7	2273.1	276.4	6.15	2.48
LT-Pt_3Al	17.65	4365.5	2273.1	2543.6	310.5	6.97	6.34
Pt	21.45	3992.1	1822.3	2053.9	240		
Pt[a]	21.45	3891.2	1820.6	2049.7	246.2	5.49	3.45
Al	2.7	6390.3	3191.4	3580.4	416.8		
Al[a]	2.7	6243.7	3260.3	3647.5	424.6	6.07	2.59
Al[b]	2.7	6401.9	3103.2	3487.3	428		

[a] Exp. in Ref. [29].
[b] Exp. in Ref. [33].

Please cite this article in press as: Feng J et al. Stability, thermal and mechanical properties of Pt_xAl_y compounds. J Mater Design (2011), doi:10.1016/j.matdes.2011.02.043

$[100] = [010]$

$[100]\, v_l = \sqrt{C_{11}/\rho}; \quad [001]\, v_{t1} = \sqrt{C_{44}/\rho}; [010]\, v_{t2} = \sqrt{C_{66}/\rho}$; (18)

$[001]$

$[001]\, v_l = \sqrt{C_{33}/\rho}; [100]\, v_{t1} = [010]\, v_{t2} = \sqrt{C_{66}/\rho}$ (19)

$[110]$

$[110]\, v_l = \sqrt{(C_{11} + C_{12} + 2C_{66})/2\rho}; \quad [001]\, v_{t1} = \sqrt{C_{44}/\rho}$;

$[1\bar{1}0]\, v_{t2} = \sqrt{(C_{11} - C_{12})/2\rho}$ (20)

Orthorhombic crystal class:

$[100]$

$[100]\, v_l = \sqrt{C_{11}/\rho}; \quad [010]\, v_{t1} = \sqrt{C_{66}/\rho}; [001]\, v_{t2} = \sqrt{C_{55}/\rho}$ (21)

$[010]$

$[010]\, v_l = \sqrt{C_{22}/\rho}; \quad [100]\, v_{t1} = \sqrt{C_{66}/\rho}; [001]\, v_{t2} = \sqrt{C_{44}/\rho}$ (22)

$[001]$

$v_l = \sqrt{C_{33}/\rho}; \quad [100]\, v_{t1} = \sqrt{C_{55}/\rho}; [010]\, v_{t2} = \sqrt{C_{44}/\rho}$ (23)

Trigonal crystal class:

$[100]$

$[100]\, v_l = \sqrt{(C_{11} - C_{12})/2\rho}; \quad [010]\, v_{t1} = \sqrt{C_{11}/\rho}$;

$[001]\, v_{t2} = \sqrt{C_{44}/\rho}$ (24)

$[001]$

$[001]\, v_l = \sqrt{C_{44}/\rho}; \quad [100]\, v_{t1} = \sqrt{C_{33}/\rho}$;

$[010]\, v_{t2} = \sqrt{C_{44}/\rho}$ (25)

where C_{ijkl} are the elastic constants; n_j and n_l are the polarization and propagation directions, respectively; ω is the phonon frequency and v is the sound velocity (v_l: the longitudinal wave of sound velocity, v_{t1}: the first transverse wave of sound velocity, v_{t2}: the second transverse wave of sound velocity). The calculated results are shown in Tables 5–8. The anisotropic properties of sound velocities indicate the elastic anisotropy in these crystals. For example, the C_{11}, C_{22} and C_{33} determine the longitudinal sound velocities along [1 0 0], [0 1 0] and [0 0 1] directions, respectively, and C_{44}, C_{55} and C_{66} correspond to the transverse modes.

Table 5
The anisotropic sound velocities of cubic Pt_xAl_y binary compounds, and the unit of velocity (v) is km/s.

Direction	[1 0 0]		[1 1 0]			[1 1 1]	
	[1 0 0] v_l	[0 0 1] $v_{t1,2}$	[1 1 0] v_l	[1 1 0] v_t	[0 0 1] v_t	[1 1 1] v_l	[11$\bar{2}$] $v_{t1,2}$
$PtAl_2$	5.450	3.050	5.558	4.029	3.050	5.593	2.917
PtAl	5.464	2.920	5.364	4.383	2.920	5.330	3.041
β	4.964	2.500	4.889	3.737	2.500	4.864	2.596
HT-Pt_3Al	4.358	2.036	4.379	2.815	2.036	4.386	2.006
Pt	4.090	1.704	3.965	2.797	1.704	3.922	1.891
Pt	4.038	1.686	3.868	2.893	1.686	3.810	1.933
Al	6.289	3.295	6.417	4.297	3.295	6.459	3.126
Al	6.116	3.388	6.280	4.346	3.388	6.334	3.182
Al	6.295	3.220	6.441	4.128	3.220	6.488	3.023

Table 6
The anisotropic sound velocities of tetragonal Pt_xAl_y binary compounds, and the unit of velocity (v) is km/s.

Direction	[1 0 0]			[0 0 1]			[1 1 0]		
	[1 0 0] v_l	[0 0 1] v_{t1}	[0 1 0] v_{t2}	[0 0 1] v_l	[1 0 0] v_{t1}	[0 1 0] v_{t2}	[1 1 0] v_l	[0 0 1] v_{t1}	[1$\bar{1}$0] v_{t2}
Pt_8Al_{21}	5.592	3.047	2.825	5.226	2.825	2.825	5.493	3.047	3.012
LT-Pt_3Al	4.416	2.141	2.636	4.263	2.636	2.636	4.721	2.141	2.041

Table 7
The anisotropic sound velocities of orthorhombic Pt_xAl_y binary compounds, and the unit of velocity (v) is km/s.

Direction	[1 0 0]			[0 1 0]			[0 0 1]		
	[1 0 0] v_l	[0 1 0] v_{t1}	[0 0 1] v_{t2}	[0 1 0] v_l	[1 0 0] v_{t1}	[0 0 1] v_{t2}	[0 0 1] v_l	[1 0 0] v_{t1}	[0 1 0] v_{t2}
Pt_5Al_3	4.311	2.106	2.396	4.318	2.106	1.949	4.329	2.396	1.949
HT-Pt_2Al	4.405	2.188	1.788	4.440	2.188	1.992	4.430	1.788	1.992
LT-Pt_2Al	4.402	2.626	2.087	4.462	2.626	2.609	4.794	2.087	2.609

Table 8
The anisotropic sound velocities of trigonal Pt_xAl_y binary compound, and the unit of velocity (v) is km/s.

Direction	[1 0 0]			[0 0 1]		
	[1 0 0] v_l	[0 1 0] v_{t1}	[0 0 1] v_{t2}	[0 0 1] v_l	[1 0 0] v_{t1}	[0 1 0] v_{t2}
Pt_2Al_3	5.973	2.859	5.440	3.241	2.859	2.859

Please cite this article in press as: Feng J et al. Stability, thermal and mechanical properties of Pt_xAl_y compounds. J Mater Design (2011), doi:10.1016/j.matdes.2011.02.043

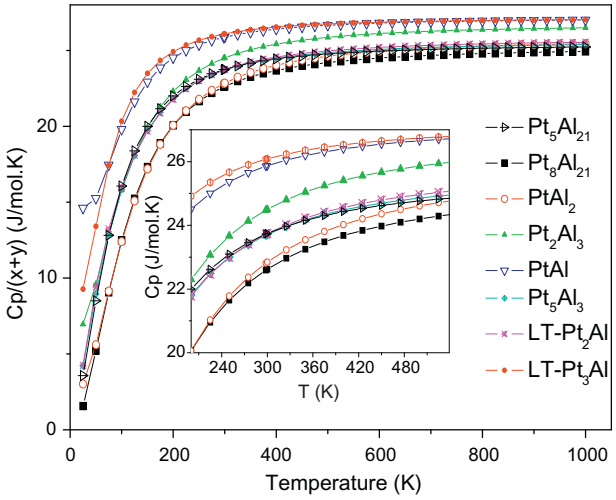

Fig. 4. The heat capacity of Pt_xAl_y binary compounds calculated using Debye's quasi-harmonic approximation.

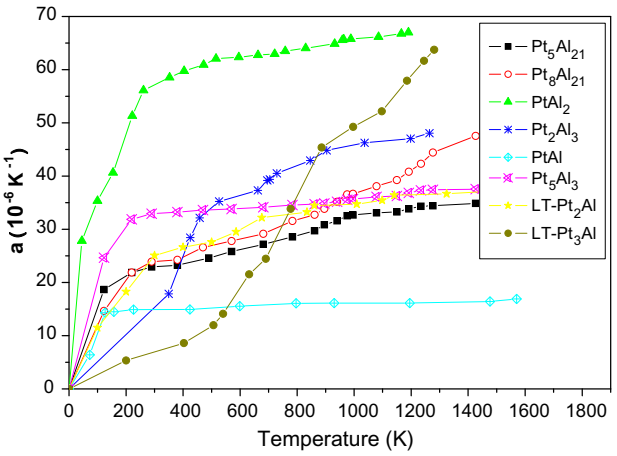

Fig. 5. The thermal expansion coefficients of Pt_xAl_y binary compounds as functions of temperatures calculated using an empirical method.

3.4. Heat capacity and thermal expansion

Firstly, the heat capacities (see Fig. 4) of the Pt_xAl_y compounds have been calculated by applying the Debye's quasi-harmonic approximation from 50 K to 1000 K. At very low temperatures, the heat capacity can be calculated using Eq. (26) [35].

$$C_P = \gamma T + \beta' T^3 \tag{26}$$

where γ is directly related to electron density of states at the Fermi surface and β' relates to phonon excitations. The heat capacity is consisted of two parts: one is attributed to electrons and the other is due to phonon excitations (or phonons). At the very high temperatures, the correlation between the heat capacity under constant pressure (C_p) and temperature (T) can be interpreted by classical rule for the ideal gas, $C_p = 3nR$, and n is the total number of atoms per formula and R is the gas constant [33]. They are calculated with the following Eqs. (27) and (28) [33],

$$\gamma = \frac{\pi^2 k_B^2 N(E_F)}{3} \tag{27}$$

$$\Theta_D^3 = \frac{12\pi^4 Rn}{5\beta} \tag{28}$$

Here Θ_D is the Debye temperature, k_B is the Boltzmann constant, R is the gas constant and $N(E_F)$ is the density of states (DOS) value at the Fermi surface. The other symbols can be found in Eqs. (23)–(25). Since γ is determined by the DOS at the Fermi level, then the compound with large DOS value will increase γ value, for instance LT-Pt_3Al and Pt_5Al_3. The heat capacity calculated using Eq. (26) is accurate when $T < \frac{1}{10}\Theta_D$, and that is below 40 K for Pt_xAl_y compounds. Above this temperature, the Debye's quasi-harmonic approximation should be applied for the calculations, and Fig. 4 shows the heat capacity of Pt_xAl_y binary compounds at higher temperatures.

The mechanical performances of the Pt_xAl_y compounds used in high temperature are mainly determined by the thermal expansion coefficient of the intermetallics. The thermal expansion coefficients (α) as a function of temperature are discussed in this section. Within the Debye approximation, the specific heat capacity at constant volume C_V^D as a function of temperature is used by Eq. (29) [33]:

$$C_V^D(T) = 9Nk\left(\frac{T}{\Theta_D}\right)^3 \int_0^{\Theta_D/T} \frac{x^4 e^x}{(e^x - 1)^2} dx \tag{29}$$

N is the Avogadro's number. In order to calculate the thermal expansion coefficient, one needs an expression for the specific heat capacity at constant volume (C_V) and the Gruoneisen constant (γ_G). They are calculated using the following Eqs. (30) and (31) [33,36],

$$\alpha(T) = \frac{1}{3} \cdot \gamma_G \cdot \frac{C_v(T)}{B \cdot V_0} \tag{30}$$

$$\gamma_G = \frac{d \ln \Theta_D}{d \ln V} \tag{31}$$

The thermal expansion coefficients as a function of temperatures for Pt_xAl_y compounds are shown in Fig. 5. For the Pt_xAl_y compounds, the thermal expansion coefficients are increased by the increasing temperature. The thermal expansion coefficients of $PtAl_2$ change dramatically below 200 K. Besides Pt_3Al, the thermal expansion coefficients of the Pt_xAl_y intermetallics vary slowly when the temperature is above 200 K. The thermal expansion properties of PtAl and Pt_5Al_3 are nearly independent of temperature above 200 K. Therefore, these compounds may easily to match with other substrates when used as bonding materials for thermal barrier coatings. However, as was already mentioned, the thermal conductivity of Al rich compounds is relatively high and the bulk modulus of them are lower than Pt rich compounds, thus Pt_5Al_3 and PtAl may superior to other phases.

4. Conclusion

In summary, the stability, mechanical, thermal properties of Pt_xAl_y intermetallics have been investigated. The cohesive energy and formation enthalpy of Pt_xAl_y compounds show that the compounds are thermodynamically stable and the bonds in the compounds are mainly metallic and covalent bonds, which are in good agreement with the experimental values. The Young's modulus of Pt_2Al_3 and PtAl are greater than other compounds, and the corresponding B/G ratios are small. The results showed C_{11}, C_{22} and C_{33} determine the longitudinal sound velocities along [1 0 0], [0 1 0] and [0 0 1] directions, respectively, and C_{44}, C_{55} and C_{66} correspond to the transverse modes. Pt rich compounds have relatively large B, G and E values when compared to Al rich compounds; the calculated sound velocities of Pt_xAl_y binary compounds are mainly determined by the density, but not the bulk modulus. The calculated Poisson's ratio varies from 0.26 for PtAl to 0.39 for Pt which is typical for metallic compound. The smallest values of PtAl and LT-Pt_3Al also imply that they may be harder than other compounds. The low thermal expansion coefficients,

Please cite this article in press as: Feng J et al. Stability, thermal and mechanical properties of Pt_xAl_y compounds. J Mater Design (2011), doi:10.1016/j.matdes.2011.02.043

medium modulus values and high melting points of the PtAl and LT-Pt_3Al intermetallics are analogous to ceramics.

Acknowledgements

Project supported by the National Natural Science Foundation of China (No. 2008CB617609, No. u0837601, No. u0837603 and No. 50874054) and Science Foundation of Kunming University of Science and Technology.

References

[1] Razumovskiy VI, Isaev EI, Ruban AV, Korzhavyi PA. Ab initio calculations of elastic properties of Pt–Sc alloys. Intermetallics 2008;16:982–7.
[2] Tian N, Zhou Z, Sun S, Ding Y, Wang ZL. Synthesis of tetra hexahedral platinum nanocrystals with high-index facets and high electro-oxidation activity. Science 2007;316:732–5.
[3] Kim HJ, Walter ME. Characterization of the degraded microstructures of a platinum aluminide coating. Mater Sci Eng A 2003;360:7–17.
[4] Osorio WR, Peixoto LC, Cante MV, Garcia A. Microstructure features affecting mechanical properties and corrosion behavior of a hypoeutectic Al–Ni alloy. Mater Des 2010;31:4485–9.
[5] Woodward C, Asta M, Trinkle DR, Lill J, Angioletti-Uberti S. Ab initio simulations of molten Ni alloys. J Appl Phys 2010;107:113522.
[6] Wolff IM, Hill PJ. Platinum metals-based intermetallics for high-temperature service. Platinum Met Rev 2000;44:158–68.
[7] Hill PJ, Yamabe-Mitarai Y, Wolff IM. High-temperature compression strengths of precipitation-strengthened ternary Pt–X alloys. Scripta Mater 2001;44:43–8.
[8] L.A.Cornish, Süss R, Watson A, Prins SN. Building a thermodynamic database for platinum-based superalloys: part I. Platinum Metals Rev 2007;51:104–15.
[9] Ferro R, Capelli R, Borsese A, Centineo G. Activity coefficients and partial molar volumes of boron in platinum–rhodium alloys, Atti AN L. Classe Sci Fis Mat Nat 1968;45:54–9.
[10] McAlister AJ, Kahan DJ. The Al–Pt (Aluminum–Platinum) system. Bull. Alloy Phase Diag. 1986;7:45–9.
[11] Oya Y, Mishima U, Suzuki T. Pt–Al and Pt–Ga phase diagram with emphasis on the polymorphism of Pt_3Al and Pt_3Ga. Z. Metallkd. 1987;78:485–90.
[12] Wu K, Jin Z. Thermodynamic assessment of the Al–Pt binary system. J Phase Equilib 2000;21:221–6.
[13] Prins SN, Cornish LA, Stumpf WE, Sundman B. Thermodynamic assessment of the Al–Ru system. CALPHAD 2003;27:79–90.
[14] Watson A, Süss R, Cornish LA. Building a thermodynamic database for platinum-based superalloys: part II. Platinum Met Rev 2007;51:189–97.
[15] de Waal H, Pretorius R. Lateral dilusion study of the Pt±Al system using the NAC nuclear microprobe. Nucl Instrum Methods B 1999;158:717–21.
[16] Chauke HR, Minisini B, Drautz R, Nguyen-Manh D, Ngoepe PE, Pettifor DG. Theoretical investigation of the Pt_3Al ground state. Intermetallics 2010;18:417–21.
[17] Bronger W, Mueller P, Wrzesien K. Zur struktur platinreicher aluminium–platin–legierungen-the structure of platinum-rich aluminium/platinum alloys. Zeitschrift fuer Anorganische and Allgemeine Chemie 1997;623:362–8.
[18] Hohenberg P, Kohn W. Inhomogeneous electron gas. Phys Rev 1964;136:864.
[19] Segall MD, Lindan PJD, Probert MJ. First-principles simulation: ideas, illustrations and the CASTEP code. J Phys Condens Matter 2002;14:2717–44.
[20] Kresse G, Joubert D. From ultrasoft pseudopotentials to the projector augmented-wave method. Phys Rev B 1999;59:1758.
[21] Perdew JP, Burke K, Emzerhof M. Generalized gradient approximation made simple. Phys Rev Lett 1996;77:3865–8.
[22] Liang YJ, Che YC, Liu XX. Manual of practical inorganic matter thermodynamics [M]. Shenyang: Northeastern University Press; 1993.
[23] Range KJ, Christl EG. Hochdrucksynthese und kristallstruktur von Pd_8Al_{21}, $Pd_8Al_{17}Si_4$ und Pt_8Al_{21}. J Less-Common Met 1988;136:277–97.
[24] Ellner M, Kattner U, Predel B. Konstitutionelle und strukturelle untersuchungen im aluminiumreichen teil der systeme Ni–Al und Pt–Al. J Less-Common Met 1982;87:305–25.
[25] Huch R, Klemm W. Das system platin–aluminium. Zeitschrift fuer Anorganische and Allgemeine Chemie 1964;329:123–35.
[26] Bhan S, Kudielka H. Ordered bcc-phases at high temperatures in alloys of transition metals and b-subgroup elements. Zeitschrift fuer Metallkunde 1978;69:333–6.
[27] Chattopadhyay TK, Schubert K. Kristallstruktur von Pt_2Al. J Less-Common Met 1976;45:79–83.
[28] Simmons G, Wang H. Single crystal elastic constants and calculated aggregate properties: a handbook. Cambridge, MA: MIT Press; 1971.
[29] Zhang Y, Han Y, Chen G, Guo J. Intermetallics structure materials. Beijing: Science Press; 2001.
[30] Söderlind P, Eriksson O, Wills JM, Boring AM. Theory of elastic constants of cubic transition metals and alloys. Phys Rev B 1993;48:5844.
[31] Song Y, Guo ZX, Yang R, Li D. A first principles study of site substitution of ternary elements in NiAl. Acta Mater 2001;49:1647–54.
[32] Gao F. Hardness estimation of complex oxide materials. Phys Rev B 2004;69:094113.
[33] Grimvall G. Thermophysical properties of materials, North Holland. Amsterdam: Elsevier B. V; 1999.
[34] Hearmon RFS. An introduction to applied anisotropic elasticity. Oxford: Oxford University Press; 1961.
[35] Lofland SE, Hettinger JD, Meehan T, Finkel P, Barsoum MW, Hug G. Electron-phonon coupling in $M_{n+1}AX_n$-phase carbides. Phys Rev B 2006;74:174501.
[36] Gibiansky LV, Torquato S. Thermal expansion of isotropic multiphase composites and polycrystals. J Mech Phys Solids 1997;45:1223–52.

Please cite this article in press as: Feng J et al. Stability, thermal and mechanical properties of Pt_xAl_y compounds. J Mater Design (2011), doi:10.1016/j.matdes.2011.02.043